Characterization of hydrosoluble fraction and oligomers in poly(vinylidene chloride) latexes by capillary electrophoresis using electrophoretic mobility modeling

Amal Ibrahim, Herve Cottet

Characterization of hydrosoluble fraction and oligomers in poly(vinylidene chloride) latexes by capillary electrophoresis using electrophoretic mobility modeling

Amal Ibrahim, Hervé Cottet*

IBMM, University of Montpellier, CNRS, ENSCM, Montpellier, France

TITLE RUNNING HEAD. Characterization of hydrosoluble oligomers in latexes by CE

* CORRESPONDING AUTHOR
Tel: +33 4 6714 3427, Fax: +33 4 6763 1046. E-mail: herve.cottet@umontpellier.fr

ABSTRACT.

The characterization of hydrosoluble oligomers in latexes is an important topic in emulsion polymerization since oligomers are suspected to be responsible for latex destabilization. In this work, the hydrosoluble fraction of poly(vinylidene chloride) latexes synthesized by emulsion polymerization of three monomers (acrylic acid, methyl acrylate, vinylidene chloride) was characterized by capillary electrophoresis (CE). CE using direct UV detection permitted to estimate residual monomers and surfactants concentrations contained in the latexes serums. Water soluble oligomers, polymerization initiator (persulfate) and other inorganic anions were detected by indirect UV detection. The oligomers content in the dry extract of serum was estimated to be about 6% (% m/m) represented mainly by 9 different compounds belonging to 3 different families. Using a semi-empirical electrophoretic mobility modeling, the charge number of these oligomers was estimated to be -2 and the molar masses were estimated in the range of ~300-550 $g.mol^{-1}$. Oligomer samples obtained by surfactant-free polymerization, with different initial monomers proportions, provided qualitatively 14 different oligomers, including the 9 oligomers previously detected in the serums. Finally, the latex was characterized (electrophoretic mobility and zeta potential) using its serum as a background electrolyte. This approach could be very useful to study the behavior of the latexes, and possibly destabilization effect, in analytical conditions very close to its real environment / applications.

Keywords: Capillary electrophoresis, indirect UV detection, latex, hydrosoluble fraction, serum, oligomers, emulsion polymerization, electrophoretic mobility modeling.

1. Introduction

Nowadays, emulsion polymerization is widely used in the synthesis of heterogeneous polymer colloids, especially when a hydrophobic monomer is involved. In this process, the hydrophobic monomer is polymerized in an aqueous phase in presence of a surfactant playing a stabilizer role [1-4]. The emulsion polymerization allows for preparing more complex nanoparticles, controlling the polymerization rate, particles concentration and molar masses as well as limiting high temperature and viscosity problems[5]. This technique is the basis of a massive global industry that is expanding due to the versatility of the reaction and the ability to control properties to produce monodisperse latex particles used in coating, paints or in sustained release drug delivery systems. Poly(vinylidene chloride) is one example of latexes finding numerous applications in pharmaceutical and food industries. It has high barrier properties (or low permeability) to water, oxygen[6] and aroma[7] due to its high degree of crystallinity[8].

The mechanism of emulsion polymerization, where water acts as a continuous medium in which initiator is soluble, relies on the oligomeric radicals entry into the latex particle [9-11]. The entry occurs when oligomers chain reaches a certain length, it becomes insoluble in the aqueous phase. Oligomers radicals may terminate in the aqueous phase to produce hydrophilic species. These hydrophilic oligomers, which are not adsorbed onto the latex particle, remain in the aqueous phaseof the latex (called the serum); together with other compounds such as salts, ionic surfactants, residual monomers, initiators, inhibitors, or degradation hydrophilic compounds. The presence of these hydrosoluble species may have a significant influence on the latex physico-chemical characteristics. It was reported that these oligomers are an important parameter affecting the polymerization process as well as the emulsion stabilization [12-16]. Several studies were focused on the characterization of hydrosoluble oligomers, especially to model the entry of radicals in emulsion polymerization. Gilbert et al. calculated values for the degree of polymerization to be reached, for entry into a latex particle, and they found 2 for

polystyrene, 7-8 for poly(vinyl acetate) and 4-5 for poly(methyl methacrylate) and poly(vinyl chloride) [13]. They also obtained, experimentally, 2 for polystyrene using isotachophoresis (ITP) [17]. Eleveld et al. used liquid chromatography to separate charged and uncharged oligomers formed during emulsion polymerization [18]. Poehlein et al. separated oligomers of low molar mass by membrane filtration and characterized them by Fourier transform infrared spectroscopy (FTIR) and mass spectrometry (MS) [19]. The same group succeeded to determine oligomer molar mass by MS and the critical size to be captured by particle to be about 5-6 monomers of vinyl acetate, which is in good agreement with their theoretical value obtained by modeling [12]. Mean values of 8-9 were obtained for methyl methacrylate by means of MS and size exclusion chromatography (SEC) [20]. Van Herk and co-workers have recently developed a semi-quantitative method for oligomer analysis by MALDI-TOF-MS giving valuable information about the molar mass distribution which were similar to SEC results [11]. Independently, SEC and IR spectroscopy were used to measure oligomer size and entry rate [21]. Many techniques, such as SEC, ^{1}H-NMR and GC, were employed by Yuan et al. to characterize oligomers in the serum of latex based on styrene, butadiene and acrylic acid copolymerization. When the proportion of the latter monomer was increased, the concentration of hydrosoluble oligomers, particle number and the polymerization rate increased [22]. Salovey and co-workers used scanning electron microscopy (SEM) for size determination and SEC for monitoring oligomers formation [23,24]. Recently, dynamic light scattering technique (DLS) was developed for the determination of monomers concentration in the latex particle [25]. On the other hand, Cottet et al. demonstrated the possibility to separate oligo(styrene sulfonate) by free solution CE [26,27]. Later, Castignolles et al. demonstrated that CE provides better resolution than SEC for the separation of oligo(acrylic acid) with separation according to their tacticity [15].

Beyond the hydrosoluble fraction, latex particles can be characterized after synthesis by different techniques. In literature, ^{1}H-NMR is often employed for composition determination, differential scanning calorimetry (DSC) as a technique for glass transition temperature (Tg) determination, DLS and SEM for size distribution estimation, and SEC for the separation and molar mass determination [23, 28-30]. FTIR and TGA (thermal gravimetric analysis) were used for the verification of grafting percentage of functional groups on the particle surface [31]. Zeta potential (ζ) is an important parameter for characterizing suspension stability. Basically, zeta potential determination requires the measurement of both electrophoretic mobility (μ_{ep}) and hydrodynamic radius (R_h), combined to theoretical or numerical equations (known as O'Brien-White-Ohshima modeling), setting the relationship between ζ, μ_{ep} and R_h [32-37]. μ_{ep} is often measured by Laser Doppler Velocimetry (LDV) while R_h is generally obtained by DLS on the same instrumentation. Alternatively, CE can be used for nanoparticle μ_{ep} determination [37-39] while Taylor dispersion analysis (TDA) [40-42] provides the R_h determination using the same CE equipment. Therefore, CE instrumentation is well adapted for zetametry of nanoparticles, providing additional information on the charge density distribution / polydispersity [43,44].

The aim of this work was the characterize PVDC (polyvinylidene chloride) latexes and their hydrosoluble fraction by CE techniques. CE methods were developed for a quantitative estimation of the hydrosoluble fraction, for the detection and characterization of hydrosoluble oligomers and for the characterization of the latex in electrophoretic conditions close to its applications.

2. Experimental section

2.1. Chemicals and samples

Dowfax 2A1 surfactant was produced by the Dow Chemical Company. Vinylidene chloride (VDC) was supplied by Fluka. Arginine was purchased from Avocado (Heysham, England).

Acrylic acid (AA), methyl acrylate (MA), ammonium persulfate, sorbic acid, boric acid, lithium hydroxide, sodium hydroxide, pyromellitic acid (1,2,4,5 benzenetetra-carboxilic acid), polyoxyethylene (23) lauryl ether (Brij 35 of M ~1198 g mol^{-1}) and hydroxypropylcellulose (HPC, M_w 10^5 g mol^{-1}) were from Sigma-Aldrich (Steinheim, Germany). Deionized water was further purified with a Milli-Q system from Millipore (Molsheim, France).

Latexes and oligomers were provided by Solvay (Tavaux, France). Non confidential information about their synthesis is reported in this section. Latexes were prepared by semi-continuous emulsion polymerization using Dowfax 2A1 as a surfactant and in the presence of a buffering agent at 4 $g.L^{-1}$(note that the chemical nature was not specified by the manufacturer). Ammonium persulfate and ascorbic acid were used as polymerization initiators. Oligomers were prepared in similar experimental conditions but in the absence of Dowfax 2A1 surfactant. Latexes and oligomers are composed of 3 monomers: VDC, MA and AA. In this work, 5 latex and 5 oligomer samples were prepared at different monomers ratios; with increasing VDC to MA proportions from latex 1 to 5 and from oligomer 1 to 5. AA proportion relative to the two other monomers was kept constant for all samples. It is worth noting that, at the end of oligomers synthesis, the residual monomers were stripped off with a rotavapor until the mass of the final product was constant.

2.2. Serum preparation

The serum of different latexes was prepared by centrifugation of latex suspensions using Sigma 3K12 instrument (6935 t/min, 5000 g, 3 × 120 min at 20 °C). Supernatants were collected after each 120 min centrifugation cycle using a micropipette and submitted to a new centrifugation cycle. After the third cycle, a trans-parent supernatant (serum) was collected and stocked at room temperature.

2.3. Dry extract determination

2 mL of serum was placed in a small hemolysis tube and frozen in liquid nitrogen. The tube was freeze dried overnight at a pressure of about 0.7 mbar and -80°C using Cryotec freeze dryer instrument (Saint Gely du Fesc, France). The serum dry extract was determined in $g.L^{-1}$ by weighing the tube before (m_0), after (m_1) the serum addition and after the freeze-drying step (m_2), according to: $1000\times(m_2 - m_0)/(m_1 - m_0)$.

2.4. Latex size determination.

The z-average particle diameter (D_z) and the dispersity factor of highly diluted samples (PDI) were measured by dynamic light scattering (DLS) (NanoZS from Malvern Instruments) at 173° at 20 °C.

2.5. Capillary electrophoresis

CE was carried out on a G1600 Agilent 3D-CE instrument (Waldbronn, Germany) equipped with a diode array detector. Fused silica (Composite Metal Services, Worcester, UK) or hydroxypropylcellulose (HPC) coated fused silica capillaries of 50 cm (41.5 cm to the UV detector) × 50 µm I.D. × 375 µm O.D., were used. The capillary temperature was set at 25°C. Data were collected at 200 nm in direct UV detection mode and at 254 nm in indirect UV detection mode.

New fused silica capillaries were conditioned by performing the following washes: 1 M NaOH for 30 min, 0.1 M NaOH for 15 min and water for 10 min. The temperature of the capillary cartridge was set at 25 °C. Between runs, fused silica capillary was flushed at 1 bar with 0.1 M NaOH for 3 min then with the BGE for 5 min. For HPC coated capillaries, the capillary was flushed, between runs, at 1 bar with water for 2 min, then with the BGE for 5 min. Electropherograms were plotted in effective mobility scale using the following equation for fused silica capillaries:

$$\mu_{ep} = \left(\frac{1}{t} - \frac{1}{t_{eo}}\right)\frac{lL}{V} \qquad (1)$$

where t is the migration time and t_{eo} is the migration time of the electroosmotic marker. V is the applied separation voltage, L is the total capillary length and l is the capillary length to the detection point. In the case of HPC coated capillaries, for which the EOF mobility is very low (typically about ~2-4 TU calculated by Vigh method [45], where TU stands for Tiselius Units, 1 TU $\equiv 10^{-9}$ m^2 V^{-1} s^{-1}), the electropherograms were converted into mobility scale using chloride ion as a mobility marker (μ_{ep} = -72.5 TU in 6 mM pyromellitic / 48 mM arginine BGE).

2.6. HPC capillary coating

Capillary coating was performed using a 5% (% m/m) HPC solution prepared at room temperature and left overnight to eliminate bubbles. The capillaries (50 µm I.D.) were filled with the polymer solution using a syringe pump at 0.03 mL/h. A stream of N_2 gas at 3 bar was used to remove the excess of HPC solution and was maintained during the immobilization process of the HPC film performed by heating the capillary in a GC oven (GC-14A, Shimadzu, France). Temperature program was: 60 °C for 10 min followed by a temperature ramp from 60°C to 140 °C at 5 °C/min and finally, 140 °C for 20 min. Before use, the coated capillaries were rinsed with water for 10 min.

2.7. Capillary electrophoresis of hydrosoluble fraction

For direct UV detection mode, a 100 mM lithium borate buffer, pH 9.2 was used. It was prepared by dissolution of 100 mM boric acid with 50 mM LiOH in water. For indirect UV detection mode, two different BGE were used. The first BGE was composed of 6 mM sorbic acid / 12 mM arginine / 5 mM Brij 35, pH 8.9 and was used for the analysis of moderately mobile species (-20 to -35 TU). The second BGE was composed of 6 mM pyromellitic acid / 48 mM arginine, pH 9.4 and was used for the analysis of highly mobile species (-35 to -75 TU).

2.8. Capillary electrophoresis of latex in its serum

Uncoated fused silica capillaries were used. The serum, prepared as previously mentioned by latex centrifugation, was used as BGE. All samples were prepared by dilution in the serum.

3. Results and discussion

3.1. Estimation of the quantity of hydrosoluble oligomers in serums

As mentioned in the Chemicals section, latexes (and thus serums) may contain different components. Among all the initial ingredients, only some of them are water soluble (AA, inorganic ions, buffering agent, Dowfax 2A1 surfactant). But the hydrosoluble fraction of the latex (serum) may also contain charged oligomers of different compositions. There are obviously no available standards for these oligomers, and their quantification is therefore a difficult task. In this work, we propose to give an estimation of their mass proportion in the hydrosoluble fraction by difference.

Hydrosoluble compounds contained in the serum were first monitored by CZE using direct UV detection. Figure 1 shows the analysis of latex 1 (100 times diluted in water), its serum and Dowfax 2A1 raw material (used as a surfactant during the synthesis), using UV detection at 200 nm in a 100 mM Li borate buffer, pH 9.2. The electropherograms are presented in mobility scale, helping the identification of the peaks observed in the latex and serum. At 200 nm, the latex particles were detected at μ_{ep} ~ -35 TU and were absent in the serum, as expected. Residual acrylic acid (AA) was only detected in the serum at μ_{ep} ~ -32 TU. Dowfax 2A1 was detected as a distribution of different species according to the number of carbons (n) in the alkyl chain of the surfactant with μ_{ep} ranging from -23 to -36 TU, and with a major peak migrating at ~ -24 TU. The chemical structure of Dowfax 2A1 is displayed in the inset of Figure 1, showing two aromatic cycles, two sulfonate groups and one alkyl chain. The higher n is, the lower the effective electrophoretic mobility is (in absolute value). In the latex sample, residual Dowfax2A1 surfactant could be observed with similar peak distribution as in Dowfax 2A1 raw material. Surprisingly, the distribution of Dowfax 2A1 surfactant was very different in serum with an enrichment of low molar mass Dowfax 2A1 molecules (see peaks 1 to 9 in the upper trace of Figure 1). This means that the sedimentation of the latex particles during centrifugation

205 tends to extract Dowfax 2A1 surfactant of higher molar mass (more hydrophobic components
206 with smaller μ_{ep}) from the aqueous phase. This extraction only happens during latex
207 sedimentation since Dowfax 2A1 distribution in latex is similar to that of Dowfax 2A1 raw
208 material. It is worth noting that this Dowfax 2A1 extraction during particles sedimentation was
209 observed for all the serum samples (1-5) as shown in Figure S1 (supporting information).
210 To quantify the Dowfax 2A1 surfactant, we studied its distribution. Starting from n=13 for
211 the main peak (μ_{ep} ~-24 TU), other peaks detected in the serum were assigned to lower n value
212 following a linear $1/\mu_{ep}$=f(n) correlation, as displayed in the inset of Figure S2 in supporting
213 information. The linearity of this correlation allows us to guess the exact number of carbons in
214 the alkyl chain compared to the n=13 peak. Such linear correlation was typically observed for
215 end-charged (macro)molecules [46]. Using this relationship, it is then possible to get the
216 surfactant distribution according to n in Dowfax 2A1 raw material and in serum. These
217 distributions (Figure S2-A in supporting information) are obtained from the electropherograms
218 by changing the variables from migration time to effective mobility, and finally, from effective
219 mobility to the n variable following the general scheme recently described [47] (see supporting
220 information for calculation details). From the chemical structure of Dowfax 2A1, one can
221 assume that the response coefficient at 200 nm is proportional to Dowfax 2A1 molar
222 concentration regardless the value of n in the alkyl chain. Therefore, distributions given in
223 Figure S2-A are molar concentration sensitive distributions. From these distributions, one can
224 determine the number- and the weight-average carbons number ($\langle n \rangle_n$ and $\langle n \rangle_w$, respectively)
225 for Dowfax 2A1 in the serum and in the raw material. The weight-average carbons number
226 $\langle n \rangle_w$=11.7 obtained for Dowfax 2A1 raw material was in good agreement with an average of
227 12 carbons obtained by NMR (see Figure S2-B), and was larger than the $\langle n \rangle_w$=9.9 obtained
228 for Dowfax 2A1 in serum. By external calibration using the Dowfax 2A1 raw material, it has

been possible to estimate the mass concentration of residual Dowfax 2A1 in serum 1 (10.8 $g.L^{-1}$), representing ~47% in mass percentage of the serumdry extract (see Table 1).

AA was quantified in the serum 1 by external calibration at 0.11 $g.L^{-1}$ corresponding to 0.5% (% m/m) of serum dry extract. The serum content in buffering agent was estimated at 4 $g.L^{-1}$ (17.5% of the serum dry extract) assuming that the buffering agent stays in the aqueous phase after centrifugation due to high hydrophilicity.

Other ions which may be found as residuals or as degradation compounds are not detected in direct UV detection. These ions such as ammonium persulfate (used as initiator), sulfate (resulting from persulfate degradation) and chloride ions (resulting from VDC degradation) could be detected using indirect UV detection (electropherograms are presented in section 3.2). Their quantification by external calibration leads to 21% of ammonium sulfate, 3% of ammonium persulfate and 5% of hydrochloric acid; all estimated as mass percentage of the dry extract of serum 1 (see Table 1). Knowing the quantity of all hydrosoluble compounds except the oligomers, the oligomers content in serum dry extract could be estimated by difference at ~6% in serum 1 dry extract. The presence of oligomers was next investigated by indirect UV detection.

3.2. Oligomers analysis by indirect UV detection (IUV) in surfactant free polymerization samples.

The detection of oligomers has been first investigated on five specific oligomer samples obtained by polymerization using the same chemical composition in VDC/MA/AA monomers as for the latexes, but without surfactant to enhance the production of oligomers in water phase. The AA amount was kept constant in order to investigate the influence of the ratio VDC / MA on the synthesis of oligomers. To cover a large range of μ_{ep}, and to minimize the electromigration distortion phenomena (EMD), two different BGE were used; based on two

254 different co-ions (chromophores or probe ions). For low mobility species (-20 to -35 TU), a
255 BGE composed of 6 mM sorbic acid (monocharged) was selected (detection at 254 nm). For
256 high mobility species (-35 to -75 TU), 6 mM pyromellitic acid (four charges) was chosen. In
257 both cases, arginine counter-ion was used to buffer the BGE at pH ~9 to ensure deprotonation
258 of weak acid (carboxylic) moieties. Brij 35 was added in sorbate BGE for reasons explained in
259 section 3.4. (Serums analysis by indirect UV detection).
260 Figure 2 displays the electropherograms obtained for the 5 oligomer solutions of different
261 VDC/MA/AA chemical compositions. Figure 2A covers the μ_{ep} region between -20 and -35 TU
262 where 9 oligomer peaks were detected in sorbate BGE. In Figure 2B, 5 other oligomers (peaks
263 10 to 14) could be identified in the pyromellitate BGE. It should be noted that the
264 electropherograms in Figure 2 were obtained for different dilution ratios as indicated on the
265 graph. Residual sulfate, persulfate and chloride ions were also identified in this region of highly
266 mobile species.

267 Regarding the quantity of oligomers present in the five samples, the sum of the time-corrected
268 peak area of peaks 1 to 9 (corrected by the dilution factor of the injected sample given in Figure
269 2) is presented in Figure 3 (black symbols) as a function of oligomers with the VDC content
270 increasing from oligomer 1 to 5. Clearly, the amount of oligomers decreases by one order of
271 magnitude with increasing mass proportion in VDC. This can be explained by the high
272 hydrophobicity of VDC (0.25% m/m solubility at 20.5 °C and 0.21% m/m at 55 °C; [48])
273 compared to MA (5% m/m solubility at 60 °C; [49]).When the amount of VDC increases in
274 the mixture of monomers, the global amount of monomers solubilized in waterdecreases.
275 Moreover, the decrease of VDC initial content increases the hydrophilicity (and water
276 solubility) of the oligomers. As illustrated in Figure S3 in supporting information, the increasing
277 opacity of the oligomers solutions is due to the increasing VDC initial content which generates
278 much hydrophobic oligomers creating more and more particles by homogeneous nucleation.

279 Qualitative comparison of the oligomer distribution between the 5 samples was performed by
280 plotting the ratio of time-corrected area of peak 9 to the sum of the time-corrected area of peaks
281 1-9 as a function of the VDC initial content (red symbols in Figure 3). The relative proportion
282 of peak 9 in the mixtures is clearly increasing with increasing initial VDC content and this
283 illustrates the change in oligomers distribution when changing the initial monomers chemical
284 composition.

285 **3.3. Characterization of oligomers using effective mobility modeling**

286 To get a better insight on oligomers characteristics, we plotted in Figure 4 the effective mobility
287 of a set of about 30 different and variously charged organic molecules taken from the literature
288 [50, 51] according to the variable:

289 $$x = \frac{\ln(1+z)}{M^{0.43}} \qquad (2)$$

290 where z is the effective charge number of the molecule (taking into account the dissociation
291 state of the solute) and M is the molar mass, following the semi-empirical dependence proposed
292 by Grossman et al. [50]. To allow the comparison between the data derived from the literature
293 and the data obtained for the studied oligomers in this work, all the mobility values were
294 corrected for the ionic strength effect to a value of 3.7 mM (corresponding to the ionic strength
295 used by Grossman et al. [50]) and at 25°C. The effective mobility values with the
296 aforementioned corrections are given in Table S1 in supporting information, including data
297 from the literature and from this work. The set of data from the literature covers a wide range
298 of charge numbers from 1 to 8 and molar masses from 132 to 4541 g.mol^{-1}. Using the linear
299 relationship displayed in Figure 4, the x values of oligomers (peaks 1-9 in Figure 2A) were
300 obtained and gathered in Table 2. These 9 oligomers are distributed according to 3 different
301 groups corresponding to different ranges of electrophoretic mobility (see Figure 2A). From the
302 x values, the molar masses were calculated assuming an oligomer charge number (z) from -1 to
303 -3 (see Table 2). It is interesting to notice that the difference in molar mass between groups

ΔM_r(I; II) and ΔM_r(II; III) are in the same order of the molar masses of the neutral monomers (M_{MA} = 86 g.mol^{-1} and M_{VDC} = 97 g.mol^{-1}) in the case of z = -2; while ΔMr between two successive groups would be too low to correspond to a monomer in the case of z = -1 (ΔM_r~35); and too high in the case of z = -3 (ΔM_r~175). Therefore, we can conclude from the semi-empirical electrophoretic mobility modeling that the oligomers (peaks 1-9) are most likely doubly charged oligomers, varying by one monomer, VDC or MA, between two successive groups. The two chemical groups that can bring the charges to the oligomers may be a sulfate moiety coming from the initiation polymerization step, and/or an acrylic acid group incorporated in the chain. Setting z = -2, the estimated molar masses of the 9 oligomers (peaks 1 to 9) can be derived from x values of Table 2 between 300 and 550 g.mol^{-1}. Putative chemical structures associated to the 9 peaks for z = -2 are proposed in Table 2.

The two charges of the first putative structure in Table 2 are attributed to a sulfate moiety coming from the initiation polymerization step, and to an acrylic acid group incorporated in the chain for oligomers initiated in the aqueous phase that terminated by transfer (to monomer) or by recombination with oligomers generated by H-abstraction. For the second putative structure in Table 2, they are attributed to two sulfate moieties for oligomers without acrylic acid, that terminated by recombination, and for the third structure, to two acrylic acid for oligomers generated by H-abstraction that terminated by recombination. The different chemical pathways leading to the different putative structures are given in Scheme S1 in SI.

Of course, such approach cannot afford formal structural determination of these oligomers; and the proposed structures should be considered as possible structures. However, using this general and relatively simple approach based on electrophoretic mobility modeling permitted to get important information on the oligomer characteristics. For instance, the degree of polymerization of the putative structures varies from 4 to 6 for oligomers in group 1, from 3 to 5 for oligomers in group 2 and from 3 to 4 for oligomers in group 3. These values are in very

329 good agreement with the z-mer values reported in literature for emulsion polymerization in the
330 case of heterogeneous nucleation [2]. The simplicity of the proposed approach should be
331 considered since peak assignment based on CE-MS coupling would not be possible using the
332 optimized BGE presented in this work due to compatibility reasons (non-volatility).

333 **3.4. Serums analysis by indirect UV detection (IUV)**

334 The experimental conditions optimized on the analysis of the surfactant-free polymerization
335 samples were applied to serums analysis. Figure 5A shows the electropherograms obtained in
336 sorbic acid/arginine buffer/Brij 35 for 5 serums of different VDC/MA/AA compositions. Brij
337 35 was used to avoid any interference between the oligomers and the residual Dowfax 2A1 by
338 reducing the effective mobility of Dowfax 2A1 surfactant which interacts with the neutral Brij
339 micelles. Comparing to Figure 2A (surfactant-free polymerization), in addition to the
340 previously mentioned 9 peaks (peaks 1 to 9), a new peak is observed between peaks 6 and 7.
341 This new peak, denoted by *, could belong to a new oligomer formed during latexes synthesis
342 in presence of Dowfax 2A1 surfactant. Furthermore, serums analysis in pyromellitic acid buffer
343 (Figure 5B) shows only 2 oligomers peaks (10 and 14), while peaks 11-13 previously observed
344 in Figure 2B are not observed here. The missing oligomers could have been preferentially
345 adsorbed by micelles or existing particles and finally completely extracted from the serum [52].
346 Other peaks observed after oligomer 14, belong to residual inorganic ions: sulfate, persulfate
347 and chloride. The quantity of these ions was estimated as previously discussed in section 3.1.,
348 and the corresponding values are given in Table 1for serum 1.
349 A qualitative comparison of the oligomers distributions in the different serums is displayed
350 in Figure 3 (inset) via the time-corrected peak area of peak 9 relative to peaks 1-9. The
351 proportion of peak 9 is increasing with increasing VDC content in the initial monomer mixture.
352 These results are similar to our observations for oligomers samples analysis and confirm that
353 oligomers distribution in serum samples is changing according to the initial monomers chemical

354 composition. On the other hand, all serum samples were analyzed at the same dilution (1/50)
355 and the sum of the time-corrected peak area of 1-9 peaks is similar for all serums. Contrary to
356 our observation for surfactant-free polymerization samples, no significant difference in
357 oligomers quantity between serums was observed. This phenomenon could be attributed to the
358 mechanism of particles nucleation which is different in presence of Dowfax 2A1. A micellar
359 nucleation occurred when Dowfax 2A1 was used whereas the nucleation was heterogeneous in
360 surfactant-free polymerization. The oligomers were adsorbed by micelles and by the resulting
361 particles in the five experiments (latexes). As the surfactant concentration was kept constant,
362 the number of formed particles, and so the surface accessible to the oligomers, was identical in
363 all cases.

364 **3.5. Study of latex electrophoretic behavior in its serum**

365 To characterize the latex in electrophoretic conditions which are the closest to the conditions
366 of fabrication / application, CZE of the latex was performed using its own serum as BGE. These
367 conditions were developed to mimic the medium in which the latex is being used. Figure 6
368 displays the electropherograms obtained for 3 latexes (3, 4 and 5) analyzed by CZE in their
369 corresponding serums. The electrophoretic mobility was determined for each latex in its serum
370 and the corresponding values are -58.5, -54.7 and -52.2 TU for latex 3, 4 and 5, respectively.
371 The heterogeneity of the electrophoretic mobility distributions can reflect both charge and size
372 dispersities of the latex sample. From the average μ_{ep} values, combined to the hydrodynamic
373 radius (R_h) determined by DLS, zeta potential (ζ) were determined by means of O'Brien-White-
374 Ohshima (OWO) modeling [32], assuming that the latexes are dense spherical objects which
375 charged in surface. For the calculation using the OWO modeling, the ionic strength of the serum
376 was evaluated at ~120 mM by taking the NaCl concentration leading to the same current
377 intensity in the same experimental conditions (capillary dimensions, voltage, temperature). This
378 is a rough estimation, but it is difficult to provide a better evaluation. Dimensionless ionic drag

coefficients of sodium and chloride ions were used in the OWO modelling, as a first approximation. For details about the method of ζ determination, one can refer to references [32, 43]. From ζ values, surface charge density (σ) and effective charge number (z_{eff}) were calculated from the following equations (see Table 3 for the numerical values) [53, 43]:

$$\sigma = \frac{2\varepsilon_0\varepsilon_r\kappa k_B T}{ze}\sinh\left(\frac{ze\zeta}{2k_B T}\right)\left[1+\frac{1}{\kappa R_h}\frac{2}{\cosh^2(ze\zeta/4k_B T)}+\frac{1}{(\kappa R_h)^2}\frac{8\ln\left[\cosh(ze\zeta/4k_B T)\right]}{\sinh^2(ze\zeta/2k_B T)}\right]^{1/2} \quad (3)$$

$$z_{eff} = \frac{4\pi\sigma R_h^2}{e} \quad (4)$$

where k_B is the Boltzmann constant ($1.38.10^{-23}$ J K^{-1}), T is the absolute temperature (K), κ is Debye-Hückel parameter, e is the elementary electric charge, ε_r is the relative electric permittivity, ε_0 is the electric permittivity of vacuum, z is the charge number of the electrolyte ions (considered as a 1:1 electrolyte here). The numerical values of σ indicate a difference in surface charge density up to about 20% between latexes in their suspensions due to the differences in their monomers initial compositions.

4. Conclusion

In this work, a quantitative estimation of the different species constituting the hydrosoluble fraction (or serum) of poly(vinylidene chloride) latexes was performed using direct and indirect UV detection in CZE. Up to 6% m/m was found for oligomer content in the serum dry extract. Since oligomers are not detected in direct UV detection, this estimation was established by difference after the quantification of the other species contained in the serum. A large part of the hydrosoluble fraction (about 47% m/m) is constituted by residual Dowfax 2A1 surfactant, of which the distribution is very different from the Dowfax 2A1 raw material. The latex particles sedimentation by centrifugation tends to extract the large molar mass Dowfax 2A1 surfactant from the aqueous phase. To visualize oligomers, indirect UV detection was implemented with two different chromophores (or probe ions). Quantitative and qualitative

differences were observed in the oligomers distributions depending on the monomers initial composition of latexes (or of the surfactant-free polymerizations). Electrophoretic mobility modeling allowed us to propose putative chemical structure based on di-charged oligomers with molar masses comprised between 300 and 550 $g.mol^{-1}$. Finally, latexes were characterized, regarding their zeta potential and effective charge, by CZE in experimental conditions close to their real environment using their own serum as BGE.

AUTHOR INFORMATION

Corresponding Authors

*herve.cottet@umontpellier.fr

Author Contributions

The manuscript was written through contributions of all authors. All authors have given approval to the final version of the manuscript.

REFERENCES

[1] P.A. Lovell,M.S. El-Aasser, Emulsion Polymerization and Emulsion Polymer; John Wiley & Sons, Inc.: Chichester, U.K., 1997.
[2]R.G. Gilbert, Emulsion polymerization, a mechanistic approach; Academic Press: London, 1995.
[3] P.C. Hiemenz, R. Rajagopalan, Principles of Colloid and Surface Chemistry; Marcel Dekker, I., Ed.; 3rd ed.; New York, 1997.
[4] I. Capek, L. Tuan,Emulsion copolymerization of methyl methacrylate with ethyl acrylate, 1. Effect of the initiator concentration on the polymerization behaviour, Macromol.Chem. 187 (1986) 2063-2072.
[5] G. Odian, La polymérisation, Principes et applications; Polytechnica, Ed.; 3rd ed.; New York, 1994.
[6] Y. Li, Z. Weng, Z. Pan, Barrier properties of vinylidene chloride methyl acrylate copolymer,Chinese J. Polym. Sci.15 (1997) 319–324.
[7] P. Delassus, G. Strandburg, B. Howell, Flavor and aroma permeation in barrier film - the effects of high-temperature and high humidity,Tappi J. 71 (1988) 177–181.
[8] R.A.Wessling,D.S. Gibbs, P.T. Delassus, B.E. Obi, B.A. Howell, Vinylidene Chloride Monomer and Polymers. Kirk-Othmer: Encyclopedia of Chemical Technology, 1997, 882–923.
[9] S.C. Thickett, R.G. Gilbert,Emulsion polymerization: State of the art in kinetics and mechanisms,Polymer 48 (2007) 6965–6991.
[10] A.M. Van Herk, Chemistry and Technology of Emulsion Polymerisation; Blackwell, Ed.; Volume 10.; UK, 2005.

[11] P. Daswani, F. Rheinhold, M. Ottink, B. Staal, A. van Herk, Method to isolate and characterize oligomers present in the aqueous phase in emulsion copolymerization, Eur. Polym. J. 48 (2012) 296–308.
[12] R.S. Kshirsagar, G.W. Poehlein, J. Appl. Radical entry into particles during emulsion polymerization of vinyl acetate,Polym. Sci. 54 (1994) 909–921.
[13] I.A. Maxwell, B.R. Morrison, D.H. Napper, R.G. Gilbert, Entry of Free Radicals into Latex Particles in Emulsion Polymerization,Macromolecules 24 (1991) 1629–1640.
[14] G. Delaittre, J. Nicolas, C. Lefay, M. Save, B. Charleux, Aqueous suspension of amphiphilic diblock copolymer nanoparticles prepared in situ from a water-soluble poly(sodium acrylate) alkoxyamine macroinitiator, Soft Matter 2 (2006) 223–231.
[15] M. Gaborieau, T.J. Causon, Y. Guillaneuf, E.F. Hilder, P. Castignolles, Molecular Weight and Tacticity of Oligoacrylates by Capillary Electrophoresis–Mass Spectrometry,Aust. J. Chem. 63 (2010) 1219–1226.
[16] R.M. Fitch,C.H. Tsai, Polymer Colloids; Ed. I, Plenum Press: New York, 1971.
[17] B.R. Morrison, I.A. Maxwell, D.H. Napper, R.G. Gilbert, J.L. Ammerdorfferb, A.L. German,Characterization of Water-Soluble Oligomers Formed during the Emulsion Polymerization of Styrene by Means of lsotachophoresis, J. Polym. Sci. Part A-1 Polym. Chem. 31 (1993) 467–483.
[18] J.T. Eleveld, H.A. Claessens, J.L. Ammerdorffer, C.A. Cramers, A.M. van Herk,Evaluation of mixed-mode stationary phases in liquid chromatography for the separation of charged and uncharged oligomer-like model compounds, J. Chromatogr. A 677 (1994) 211–227.
[19] S.T. Wang, G.W. Poehlein, Studies of water-soluble oligomers formed in emulsion copolymerization, J. Appl. Polym. Sci. 51 (1994) 593–604.
[20] B. Thomson, Z. Wang, A. Paine, G. Lajoie, A. Rudin,A mass spectrometric investigation of the water-soluble oligomers remaining after the emulsion polymerization of methyl methacrylate, J. Polym. Sci. Part A Polym. Chem. 33 (1995) 2297–2304.
[21] C. Marestin, A. Guyot, Communications to the Editor onto Latex Particles in an Emulsion, Macromolecules 9297 (1998) 1686–1689.
[22] X. Yuan, V.L. Dimonie, E.D. Sudol, M.S. El-Aasser, Toward an Understanding of the Role of Water-Soluble Oligomers in the Emulsion Polymerization of Styrene - Butadiene - Acrylic Acid . Separation and Characterization of the Water-Soluble Oligomers, Macromolecules 35 (2002) 8346–8355.
[23] J. Li, R. Salovey, "Continuous" emulsifier-free emulsion polymerization for the synthesis of monodisperse polymeric latex particles, J. Polym. Sci. Part A-Polymer Chem. 38 (2000) 3181–3187.
[24] X. Li, R. Salovey, Oligomer Formation in the Emulsifier-Free Emulsion Polymerization of Styrene,J. Polym. Sci. Part A-Polymer Chem. 38 (2000) 1323–1336.
[25] M. Abdollahi, M. Hemmati, A New Method to Determine Monomer Concentration in the Polymer Particles of Emulsion Polymerization Systems by Dynamic Light Scattering,J. Appl. Polym. Sci. 114 (2009) 1055–1063.
[26] H.Cottet, P. Gareil, From small charged molecules to oligomers: a semiempirical approach to the modeling of actual mobility in free solution,Electrophoresis 21 (2000) 1493–1504.
[27] H. Cottet, P. Gareil, O.Theodoly, C. Williams, A semi-empirical approach to the modeling of the electrophoretic mobility in free solution: Application to polystyrenesulfonates of various sulfonation rates,Electrophoresis 21 (2000) 3529–3540.
[28] S. Bhawal, D. Dhoble, S. Devi, Revisiting emulsion polymerization to produce stable, translucent, nanolatex of partially water-soluble monomers, ethylacrylate-methylmethacrylate,J. Appl. Polym. Sci. 90 (2003) 2593–2603.

[29] M. Gaborieau, H.D.E. Bruyn, S. Mange, P.Castignolles, A. Brockmeyer, R.G. Gilbert, Synthesis and Characterization of Synthetic Polymer Colloids Colloidally Stabilized by Cationized Starch Oligomers, J. Polym. Sci. 47 (2009) 1836–1852.
[30] J. Garnier, P.E.Dufils, J.Vinas, Y.Vanderveken, A.van Herk, P. Lacroix-Desmazes, Synthesis of poly(vinylidene chloride)-based composite latexes by emulsion polymerization from epoxy functional seeds for improved thermal stability, Polym. Degrad. Stab. 97 (2012) 170–177.
[31] A.Chatterjee, S.Mishra, Novel synthesis with an atomized microemulsion technique and characterization of nano-calcium carbonate (CaCO3)/poly(methyl methacrylate) core–shell nanoparticles,Particuology 11 (2013) 760–767.
[32] H. Ohshima, Approximate Analytic Expression for the Electrophoretic Mobility of a Spherical Colloidal Particle, J. Colloid Interface Sci.239 (2001) 587–590.
[33] K.Kimura, S.Takashima, H.Ohshima, Molecular Approach to the Surface Potential Estimate of Thiolate-Modified Gold Nanoparticles,J. Phys. Chem. B 106 (2002) 7260–7266.
[34] S.M. Agnihotri, H. Ohshima, H. Terada, K. Tomoda, K. Makino, Electrophoretic mobility of colloidal gold particles in electrolyte solution, Langmuir 25 (2009) 4804–4807.
[35] U.Pyell, CE characterization of semiconductor nanocrystals encapsulated with amorphous silicium dioxide, Electrophoresis 29 (2008) 576–589.
[36] U. Pyell, W. Bücking, C. Huhn, B. Herrmann, A. Merkoulov, J. Mannhardt, H. Jungclas, T. Nann, Calibration-free concentration determination of charged colloidal nanoparticles and determination of effective charges by capillary isotachophoresis,Anal. Bioanal. Chem. 395 (2009) 1681–1691.
[37] N. Anik, M. Airiau, M.P. Labeau, W. Bzducha, H. Cottet, Characterization of copolymer latexes by capillary electrophoresis,Langmuir 26 (2010) 1700–1706.
[38] S.P. Radko, M. Stastna, A. Chrambach, Capillary zone electrophoresis of sub-µm-sized particles in electrolyte solutions of various ionic strengths: Size-dependent electrophoretic migration and separation efficiency,Electrophoresis 21 (2000) 3583–3592.
[39] F. Oukacine, A. Morel, H. Cottet, Characterization of carboxylated nanolatexes by capillary electrophoresis,Langmuir 27 (2011) 4040–4047.
[40]M.S. Bello, R. Rezzonico, P.G. Righetti, Use of taylor-aris dispersion for measurement of a solute diffusion coefficient in thin capillaries,Science 266 (1994) 773–776.
[41] H. Cottet, J.P. Biron, M. Martin, Taylor dispersion Analysis of mixtures,Anal. Chem. 79 (2007) 9066–9073.
[42] F. d'Orlyé, A. Varenne, P. Gareil, Determination of nanoparticle diffusion coefficients by Taylor dispersion analysis using a capillary electrophoresis instrument, J. Chromatogr. A 1204 (2008) 226–232.
[43] A. Ibrahim, H. Ohshima, S.A. Allison, Determination of effective charge of small ions, polyelectrolytes and nanoparticles by capillary electrophoresis,J. Chromatogr. A 1247 (2012) 154–164.
[44] U. Pyell, A.H. Jalil, C. Pfeiffer, B. Pelaz, W.J. Parak, Characterization of gold nanoparticles with different hydrophilic coatings via capillary electrophoresis and Taylor dispersion analysis. Part I: determination of the zeta potential employing a modified analytic approximation, J. Colloid Interface Sci.450 (2015) 288–300.
[45] B. A. Williams, G. Vigh, Fast, Accurate Mobility Determination Method for Capillary Electrophoresis, Anal. Chem. 68 (1996) 1174-1180.
[46] W.N.Vreeland, C. Desruisseaux,A.E. Karger,G. Drouin, G.W. Slater, A.E. Barron,Molar Mass Profiling of Synthetic Polymers by free-solution Capillary electrophoresis of DNA-Polymer Conjugates,Anal. Chem. 73 (2001) 1795–1803.

[47] J. Chamieh, M. Martin, H. Cottet, Quantitative analysis in capillary electrophoresis: transformation of raw electropherograms into continuous distributions. Anal. Chem. 87 (2015) 1050–1057.
[48] P.T. Delassus, D.D. Schmidt,Solubilities of vinyl chloride and vinylidene chloride in water, J. Chem. Eng. Data 26 (1981) 274–276.
[49] Y. Chen, S. Sajjadi, Particle formation and growth in ab initio emulsifier-free emulsion polymerisation under monomer-starved conditions,Polymer 50 (2009) 357–365.
[50] P.D. Grossman, J.C. Colburn, H.H. Lauer, A semiempirical Model for the Electrophoretic Mobilities ofpeptides in free-solution capillary electrophoresis. Anal. Biochem. 179 (1989) 28–33.
[51] R. Plasson, H. Cottet, Determination of homopolypeptide conformational changes by the modeling of electrophoretic mobilities. Anal. Chem. 79 (2007) 3020–3020.
[52] P. Daswani, Entry in Emulsion Copolymerization, PhD Thesis, Technische Universiteit Eindhoven, 2012.
[53] K. Makino, H. Ohshima, Electrophoretic mobility of a colloidal particle with constant surface charge density. Langmuir 26 (2010) 18016.

551 FIGURE CAPTIONS

552 Figure 1. Mobility scale electropherograms for latex 1, its serum and Dowfax 2A1 raw material,
553 each peak is assigned by the number of carbon atoms in the alkyl chain (n = 0-13). The inset
554 shows the Dowfax 2A1 structure. BGE: 100 mM Li borate buffer, pH 9.2. Experimental
555 conditions: Fused silica capillary 50 cm (41.5 cm to the detector) × 50 µm I.D. × 375 µm O.D.
556 Separation voltage: +10 kV with 10 mbar co-pressure. Hydrodynamic injection: 50 mbar, 5 s.
557 Temperature: 25 °C. AA stands for acrylic acid.

558 Figure 2. Mobility scale electropherograms for oligomers of different VDC/MA/AA
559 compositions with VDC content increasing from oligomer 1 to 5. (A) Electropherograms in the
560 range of -20 and -35 TU obtained in BGE 6 mMsorbic acid / 12 mM arginine / 5 mMBrij 35,
561 pH 8.9. (B) Electropherograms, in the mobility range of -45 and -75 TU, obtained in BGE 6
562 mMpyromellitic acid / 48 mM arginine, pH 9.4. Experimental conditions: HPC coated capillary
563 50 cm (41.5 cm to the UV detector) × 50 µm I.D. × 375 µm O.D. Separation voltage: -30 kV.
564 Hydrodynamic injection: 50 mbar, 5 s. Temperature: 25 °C. Samples were prepared by dilution
565 of the stock solutions with water. Dilutions are indicated on each electropherogram. Oligomers
566 groups I to III are indicated on graph 2A.

567 Figure 3. Quantitative (left) and qualitative (right) comparison between different oligomer
568 distributions in surfactant free polymerization samples (■, ●) or in serum displayed in the inset
569 (▼). (■) Sum of the time-corrected peak area of peaks 1-9 in surfactant free polymerization
570 samples. (●) Relative time-corrected peak area of peak 9 in surfactant free polymerization
571 samples. Relative time-corrected peak area of peak 9 in serums of emulsion polymerization
572 samples (▼).

573 Figure 4. Relationship between the electrophoretic effective mobility μ_{ep} and the x parameter
574 (Eq. 2) for variously charged organic molecules (peptides) taken from the literature [48,49] and

for the oligomers of this work. Numerical values used to plot this figure are given in supporting information (Table S1).

Figure 5. Mobility scale electropherograms for serums of different VDC/MA/AA compositions with VDC content increasing from serum 1 to 5. BGE: (A) 6 mM sorbic acid / 12 mM arginine / 5 mM Brij 35, pH 8.9, (B) 6 mM pyromellitic acid / 48 mM arginine, pH 9.4. Experimental conditions: HPC coated capillary 50 cm (41.5 cm to the UV detector) × 50 µm I.D. × 375 µm O.D. Separation voltage: -30 kV. Hydrodynamic injection: 50 mbar, 5 s. Temperature: 25 °C. All samples were prepared by 50 fold dilution of the stock solutions with water. AA stands for acrylic acid.

Figure 6. Mobility scale electropherograms for latexes 3, 4 and 5 analyzed in BGE composed of their serums 3, 4 and 5, respectively. Experimental conditions: fused silica capillary 50 cm (41.5 cm to the UV detector) × 50 µm I.D. × 375 µm O.D. Separation voltage: -10 kV. Hydrodynamic injection: 50 mbar, 5 s. Temperature: 25 °C. Samples were prepared by dilution of the latex suspension in its own serum. Dilution factors are indicated on each electropherogram.

Figure1

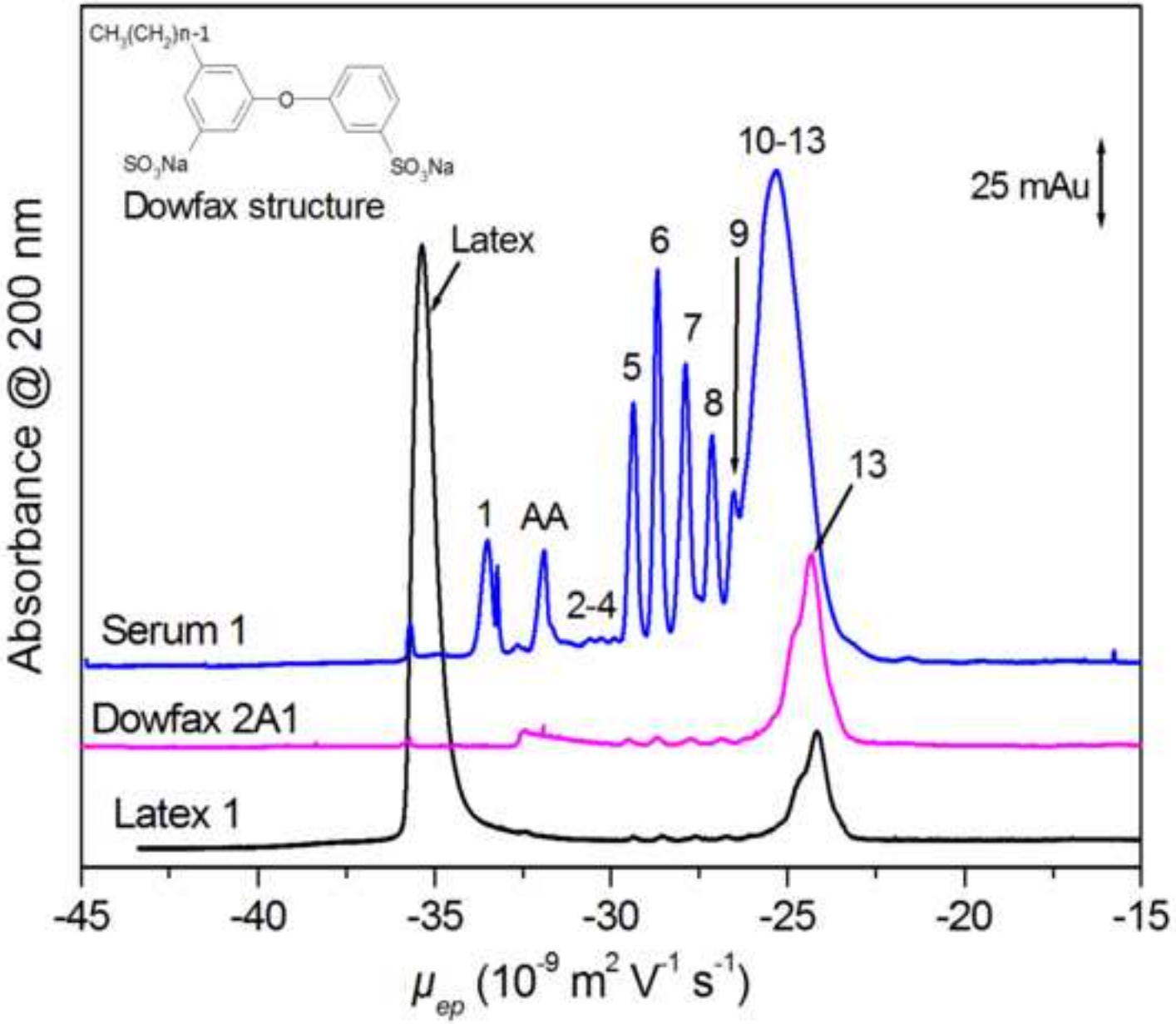
CH3(CH2)n-1
SO3Na
SO3Na
Dowfax structure
Latex
1
AA
2-4
5
6
7
8
9
10-13
13
25 mAu
Serum 1
Dowfax 2A1
Latex 1
Absorbance @ 200 nm
-45
-40
-35
-30
-25
-20
-15
μep (10-9 m2 V-1 s-1)

Figure2A

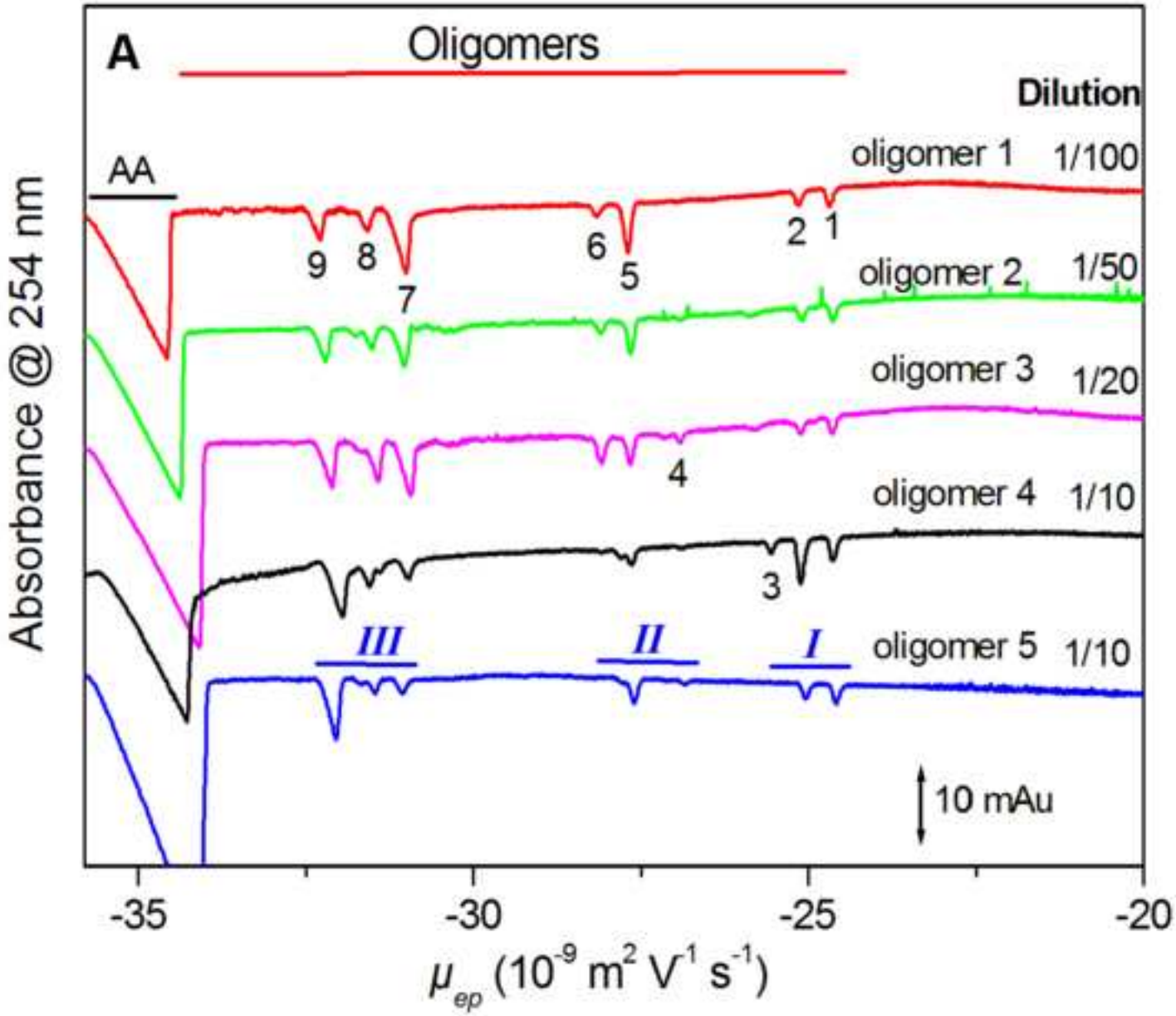
A
Oligomers
Dilution
AA
oligomer 1 1/100
oligomer 2 1/50
oligomer 3 1/20
oligomer 4 1/10
oligomer 5 1/10
9
8
7
6
5
4
3
2
1
III
II
I
10 mAu
Absorbance @ 254 nm
-35
-30
-25
-20
μ_{ep} (10^{-9} m^2 V^{-1} s^{-1})

Figure2B

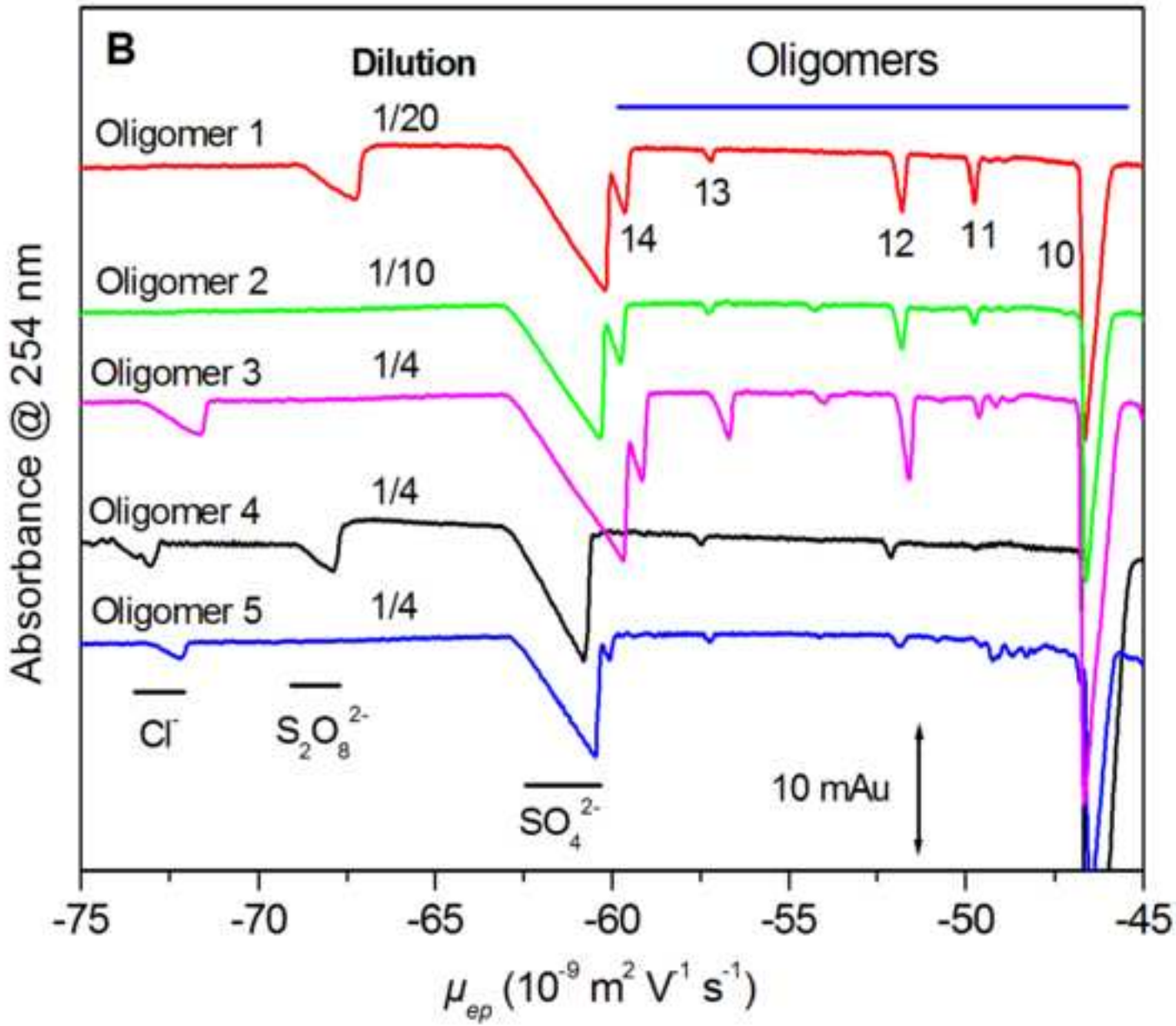
B
Dilution
Oligomers
Oligomer 1
1/20
Oligomer 2
1/10
Oligomer 3
1/4
Oligomer 4
1/4
Oligomer 5
1/4
14
13
12
11
10
Cl-
S2O8 2-
SO4 2-
10 mAu
Absorbance @ 254 nm
-75
-70
-65
-60
-55
-50
-45
μep (10-9 m2 V-1 s-1)

Figure3

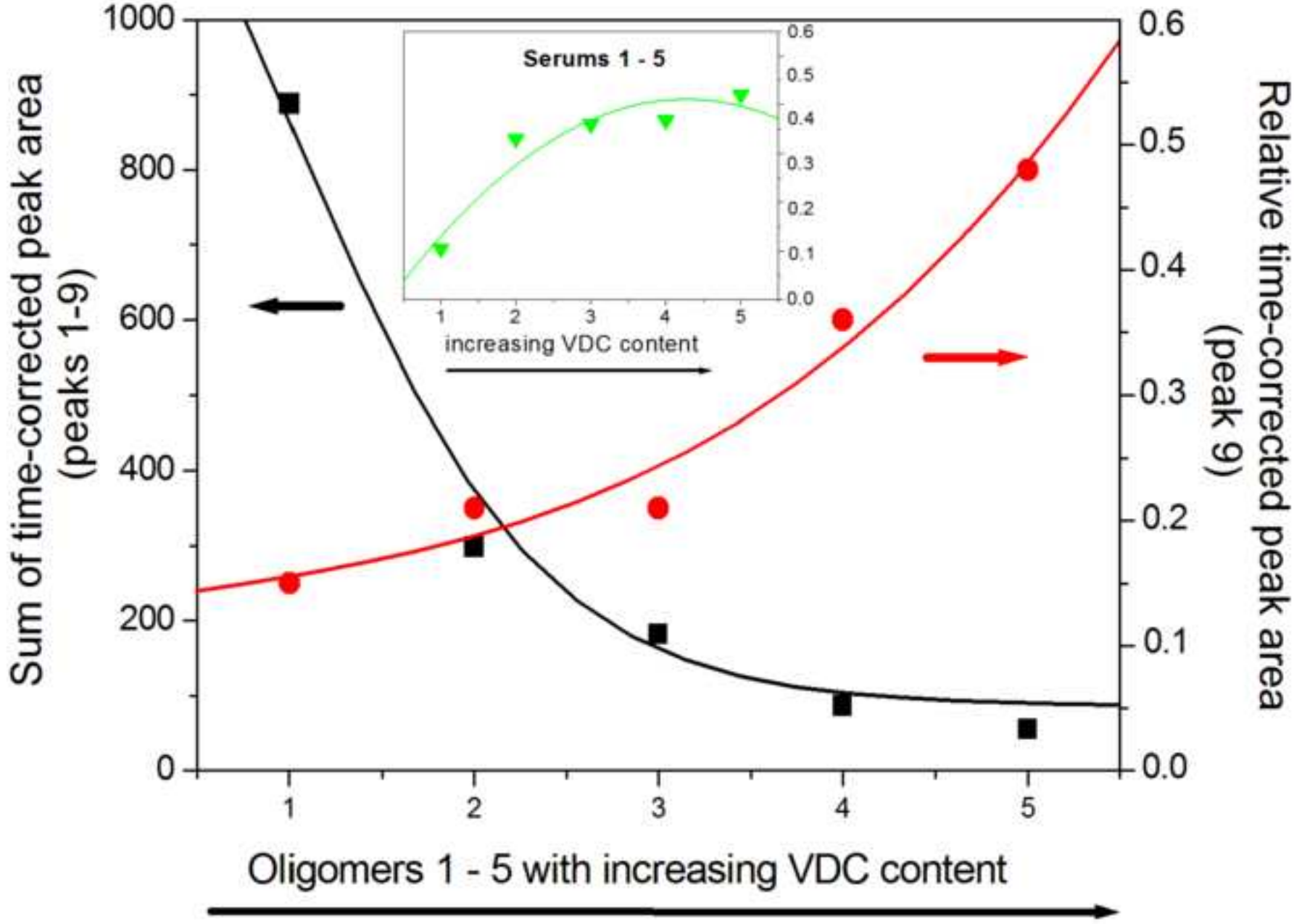
Sum of time-corrected peak area
(peaks 1-9)
Relative time-corrected peak area
(peak 9)
Oligomers 1 - 5 with increasing VDC content
Serums 1 - 5
increasing VDC content
0
200
400
600
800
1000
0.0
0.1
0.2
0.3
0.4
0.5
0.6
1
2
3
4
5

Figure4

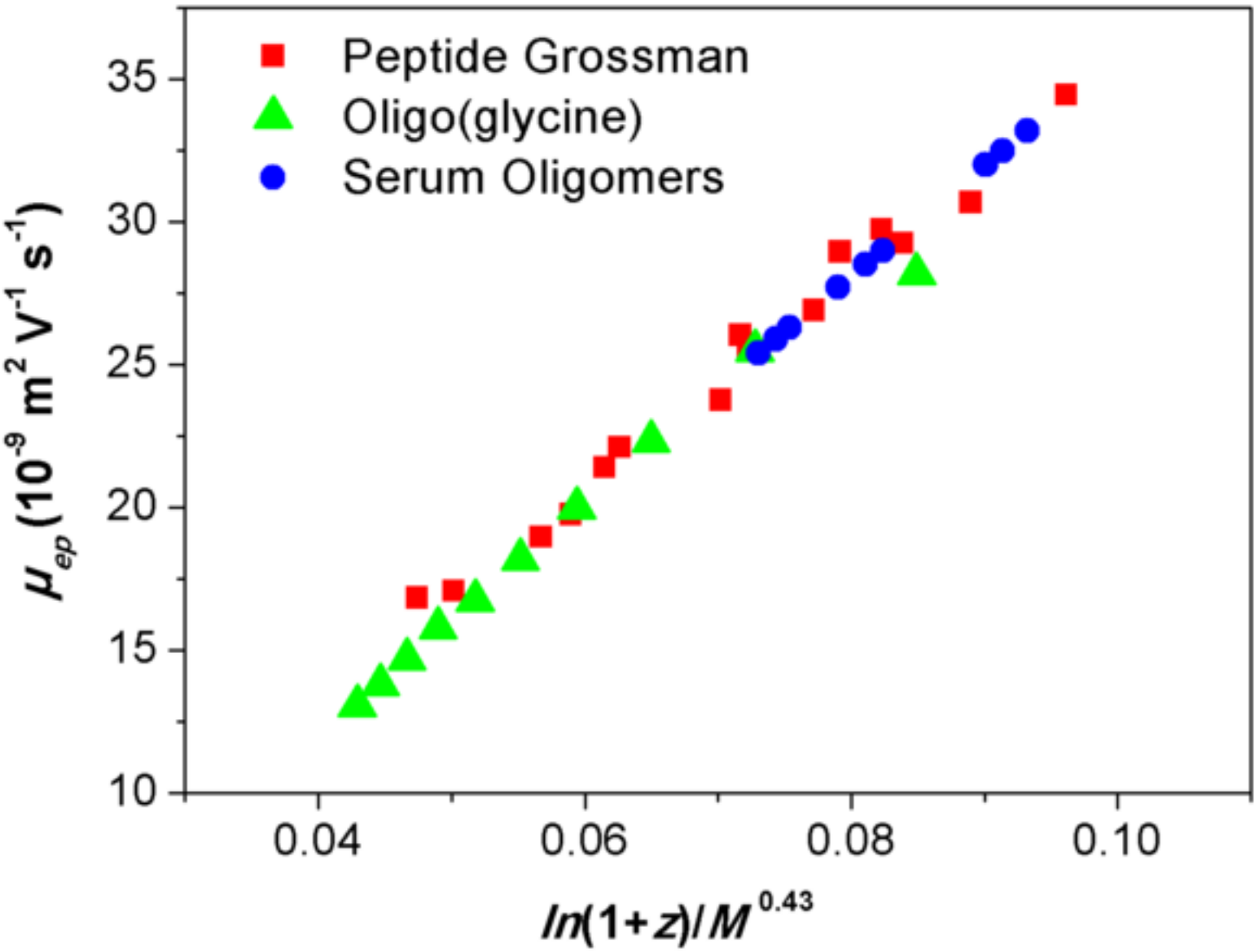
Peptide Grossman
Oligo(glycine)
Serum Oligomers
35
30
25
20
15
10
0.04
0.06
0.08
0.10
μ_{ep} (10^{-9} m^2 V^{-1} s^{-1})
$ln(1+z)/M^{0.43}$

Figure5A

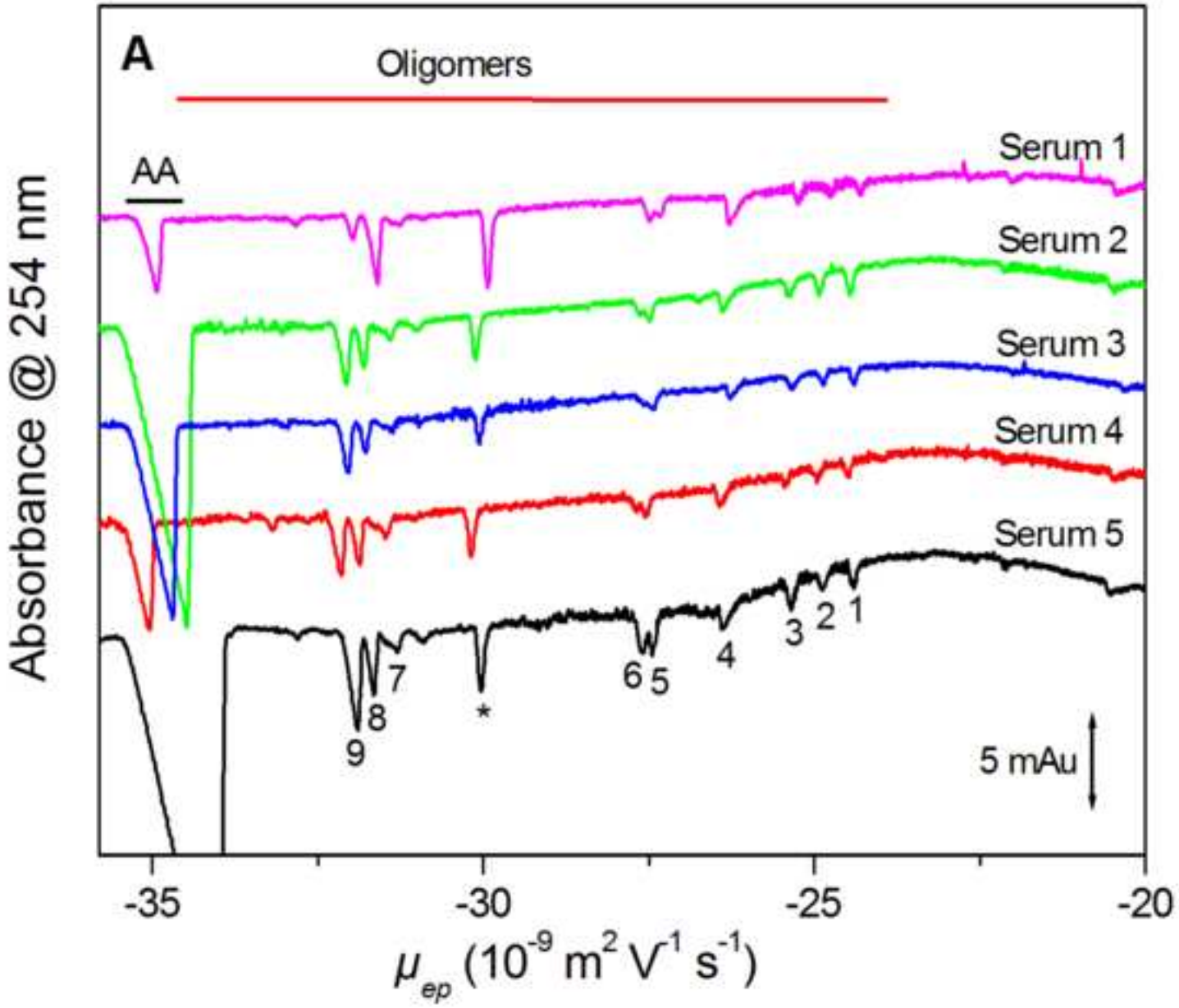
A
Oligomers
AA
Serum 1
Serum 2
Serum 3
Serum 4
Serum 5
Absorbance @ 254 nm
1
2
3
4
5
6
7
8
9
*
5 mAu
-35
-30
-25
-20
μ_{ep} (10^{-9} m^2 V^{-1} s^{-1})

Figure5B

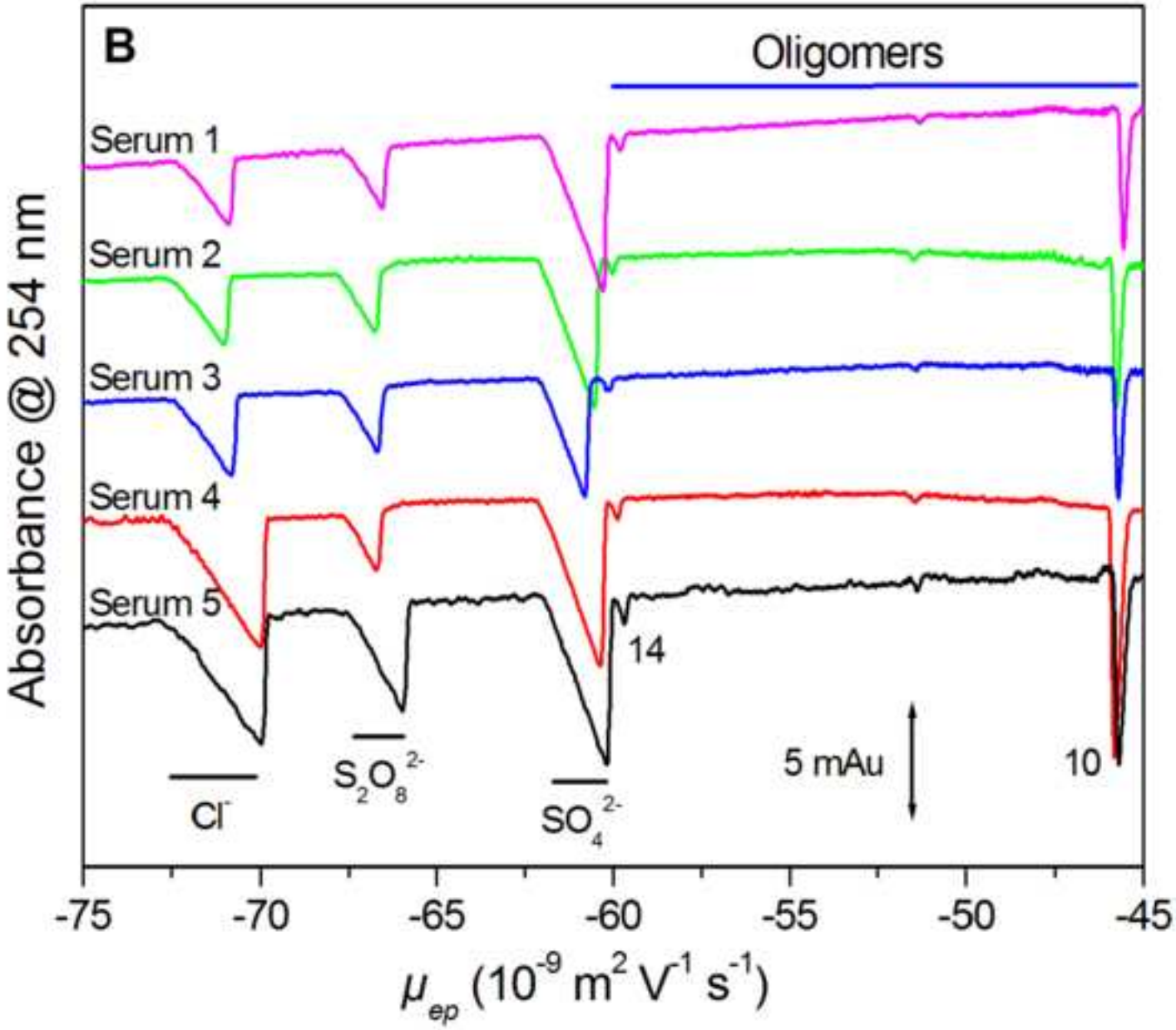
B
Oligomers
Serum 1
Serum 2
Serum 3
Serum 4
Serum 5
14
10
5 mAu
Cl-
S2O8 2-
SO4 2-
Absorbance @ 254 nm
-75
-70
-65
-60
-55
-50
-45
μep (10-9 m2 V-1 s-1)

Figure6

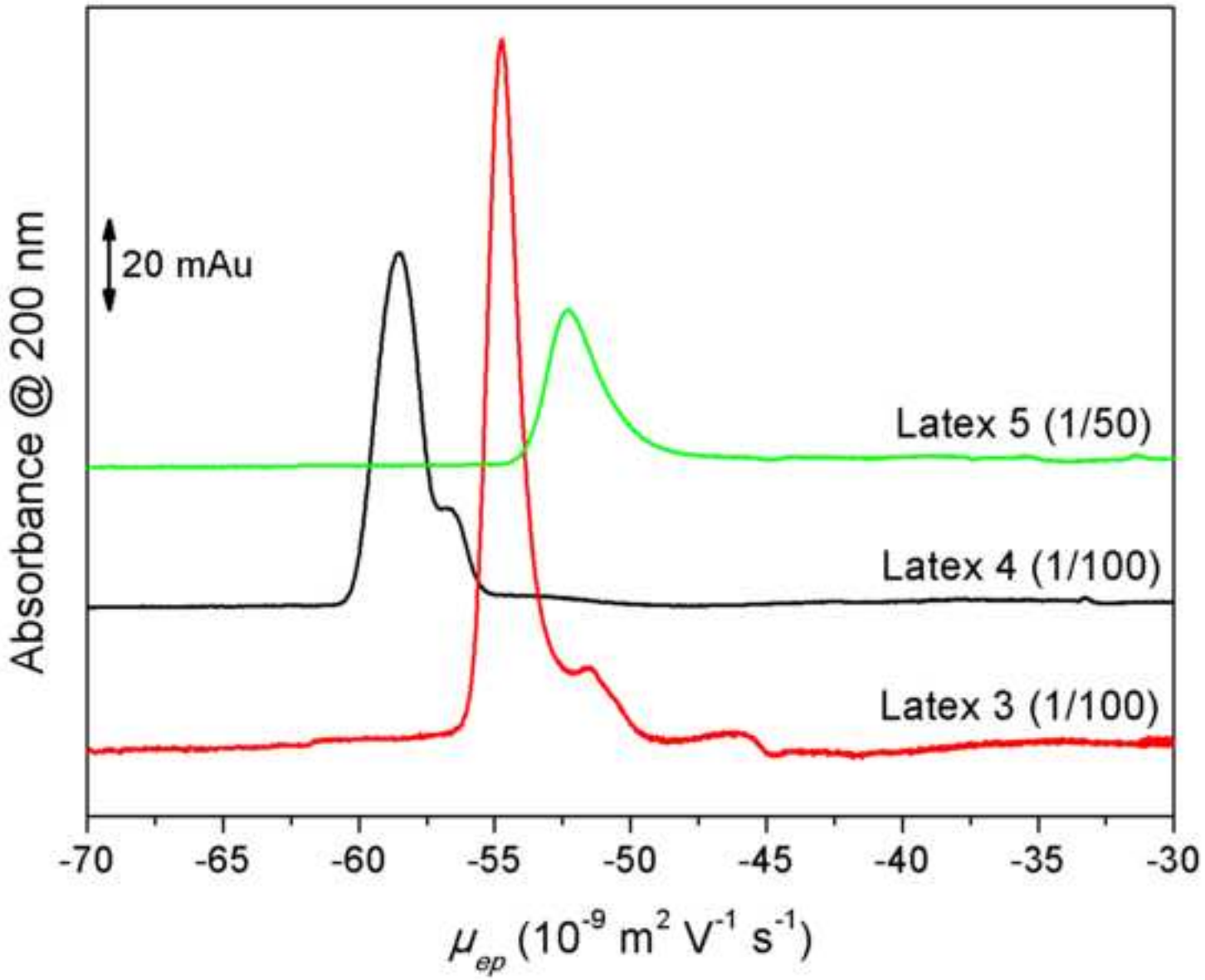
Absorbance @ 200 nm
20 mAu
Latex 5 (1/50)
Latex 4 (1/100)
Latex 3 (1/100)
-70
-65
-60
-55
-50
-45
-40
-35
-30
μ_{ep} (10^{-9} m^2 V^{-1} s^{-1})

Table1

Table 1. Estimation of the quantity of hydrosoluble oligomers in serum 1 containing 23 $g.L^{-1}$ of dry extract (% m/m). Mass concentrations (C_m) and mass percentage (% m/m) are presented for the different components of the serum: buffering agent, sulfate (SO_4^{2-}), persulfate ($S_2O_8^{2}$), chloride (Cl^-), acrylic acid (AA) and Dowfax 2A1. Oligomers quantity was estimated by difference.

	C_m ($g.L^{-1}$)	% m/m [a]	RSD [e]
Buffering agent[b]	4	17.5	N/A
SO_4^{2-} [c]	4.8	21	1.5%
$S_2O_8^{2-}$ [c]	0.7	3	1.1%
Cl^-[d]	1.1	5	1.0%
AA[d]	0.11	0.5	0.2%
Dowfax 2A1 in serum 1	10.8	47	3.1%
Oligomers in serum 1	1.5	6	N/A

[a] Mass percentage of the serum dry extract. [b] Quantity estimated assuming that the introduced quantity (4 g/L) of the buffering agent remains in aqueous phase. [c] Quantity estimated as ammonium salts by CE using external calibration. [d] Mass estimated as HCl and as CH_2=CHCOOH for AA by CE using external calibration; AA stands for acrylic acid. [e] RSD relative standard deviation determined on 3 repetitions; N/A stands for not applicable.

Table2

Table 2. x values for the water soluble oligomers determined from the μ_{ep} = f(ln(1+z)/$M^{0.43}$) correlation displayed in Figure 4 and the corresponding predicted molar masses M_r according to the possible charge number z (from -1 to -3). Putative chemical structures with the corresponding exact molar masses proposed for z = -2 (n (resp. m) is the number of VDC monomers (resp. MA monomers) in the oligomer). The three groups of oligomers (denoted I, II and III) correspond to different groups of peaks (from peak 1 to peak 9) having different effective mobility ranges.

	Oligomer	x	M_r (z = -1)		M_r (z = -2)		M_r (z = -3)		Putative chemical structure (z=-2)		
									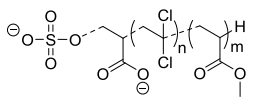 (n; m; M_r)	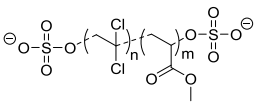 (n; m; M_r)	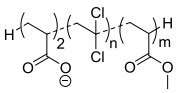 (n; m; M_r)
Group I	Peak 1	0.0730	187		547		939		(3; 1; 544), (4; 0; 555)	(1; 3; 547)	-
	Peak2	0.0743	180		525		902		(1; 3; 522), (2; 2; 533)	(0; 4; 536)	(4; 0; 530), (3; 1; 519)
	Peak 3	0.0754	174	ΔM_r(I; II) =32	508	ΔM_r(I; II)=94	873	ΔM_r(I; II)=161	(0; 4; 511)	-	(2; 2; 508), (1; 3; 497)
Group II	Peak4	0.0790	156		456		783		(3; 0; 458), (2; 1; 447)	(1; 2; 461), (0; 3; 450)	-
	Peak 5	0.0811	147		429		737		(0; 3; 425), (1; 2; 436)	-	(3; 0; 433), (2; 1; 422)
	Peak 6	0.0824	142	ΔM_r(II; III) =38	414	ΔM_r(II; III)=109	711	ΔM_r(I; III)=188	-	-	(1; 2; 411), (0; 3; 400)
Group III	Peak7	0.0901	115		336		576		(0; 2; 339)	-	(2; 0; 336), (1; 1; 325)
	Peak8	0.0914	111		325		558		-	-	(1; 1; 325)
	Peak 9	0.0932	106		310		533		-	-	(0; 2; 314)

Table 3. Characterization of latexes 3, 4 and 5 in their own serum (used as background electrolyte, BGE).

Sample	*BGE* [a]	μ_{ep} [b]	R_h [c]	ζ_{OWO} [d]	σ [e]	z_{eff} (10^{+4}) [f]
Latex 3	Serum 3	-54.7	67	-0.075	-0.0849	-2.99
Latex 4	Serum 4	-58.5	88	-0.080	-0.0943	-5.74
Latex 5	Serum 5	-52.2	55	-0.072	-0.0797	-1.89

[a] Serums prepared by latex centrifugation as mentioned in section "serum preparation" in the experimental part. [b] **e**ffective mobility in 10^{-9} m^2 V^{-1} s^{-1}. [c] hydrodynamic radius in nm, determined by DLS. [d] zeta potential in V, determined using O'Brien-White-Ohshima modeling [32] taking an ionic strength of 120 mM and ionic drag coefficients of sodium and chloride ions in OWO modelling. [e] surface charge density in (C m^{-2}) calculated using equation (3). [f] effective charge number calculated using equation (4). Experimental conditions as in Figure 6.